



Mechanistic Investigation of Methanol Oxidation on Au/TiO₂: A Combined DRIFT and DFT Study

G. D. Belletti¹ · E. Colombo¹ · N. Cabana¹ · P. Quaino¹ · S. Collins²

Accepted: 13 April 2022 / Published online: 10 May 2022

© The Author(s), under exclusive licence to Springer Science+Business Media, LLC, part of Springer Nature 2022

Abstract

The mechanism of methanol oxidation on a Au/TiO₂ catalyst was investigated by combining in situ modulation-excitation diffuse reflectance infrared spectroscopy (MES-DRIFT) with periodic density functional theory (DFT). Adsorbed reaction intermediates and spectators were identified. Methanol dissociatively adsorbs as a methoxy (CH₃O) species on the titania surface, and stepwise oxidizes to formate, carboxyl and CO, carbonates and CO₂ at the Au/TiO₂ interface. The role of the metal-support interface is clearly observed experimental and theoretically according to a metal–Au-assisted Mars van Krevelen mechanism. Energy barriers were calculated for each elementary step, and the methoxy oxidation was found to be the rate-limiting step in the proposed scenario.

Keywords Volatile organic compounds · Combustion · Reaction pathway · In situ infrared · DFT

1 Introduction

Volatile organic compounds (VOCs) are low molecular weight organic molecules with high vapor pressure and low water solubility. These are the most common human-made pollutants produced by a variety of industrial processes, such as the manufacture of chemicals, polymer synthesis, paintings, pharmaceuticals and by inefficient burning of fossil fuels [1]. VOCs typically are industrial solvents, such as hydrocarbons, esters and oxygenates (methyl tert-butyl ether (MTBE), methanol, etc.). Since 1990, the Environmental Protection Agency (EPA) includes methanol in the group of VOCs, being necessary the development of processes for its abatement.

It is well known that methanol is environmentally important due to its presence in paint solvents, such as thinner, and its massive use in the industry for the biodiesel (fatty acid methyl ester, FAME) production. Therefore, catalytic devices capable of controlling VOCs with minimal energy

cost for air purification are currently under improvement. In this context, the possibility of removing VOCs by combustion using catalysts based on gold nanoparticles supported on reducible oxides has been intensely studied due to their high activity to catalyze oxidation reactions at low temperature [2]. For instance, gold catalysts supported on reducible metal oxides, such as CeO₂ or TiO₂, perform the complete oxidation of solvents, e.g. methanol, toluene, propene, benzene and ethyl acetate, at low temperature [3–6]. It has been suggested that the metal-support sites play a crucial role. Specifically, for CO oxidation on Au/TiO₂ catalyst, several reaction pathways have been proposed, where the most accepted ones are those involving Au–O–Ti dual sites at the interface of the metal particle [7–12].

Up to now, the most comprehensive spectroscopic investigation on methanol oxidation on gold-supported catalysts, particularly Au/CeO₂ and Au/TiO₂, has been carried out by Daturi and co-workers [13, 14]. Additional experimental and theoretical studies focused on explaining the reaction mechanism of the total oxidation of methanol can be found in [15–18]. In general, adsorbed species such as methoxy, formate, carbonate and CO have been identified as reaction intermediates. However, in spite of the reported reaction mechanisms, details elucidating reaction intermediates and spectators, and particularly the role of the metal-support sites are still unclear. Hence, it is of paramount importance to investigate the reaction mechanism at a molecular level

✉ P. Quaino
pquaino@fiq.unl.edu.ar

¹ Instituto de Química Aplicada del Litoral (UNL-CONICET), FIQ-UNL, 3000 Santa Fe, Argentina

² Instituto de Desarrollo Tecnológico para la Industria Química, INTEC (UNL-CONICET), 3000 Santa Fe, Argentina

taking into account the metal-support interface and the reaction conditions to improve the catalyst design. In this context, the present paper is focused on theoretical and in situ infrared studies to shed light into the reaction path of methanol oxidation on a Au/TiO₂ catalyst.

2 Experiments

2.1 Synthesis of the Catalyst

Gold supported on TiO₂ (rutile) catalyst was prepared by deposition-precipitation with urea (DPU) using H₂AuCl₄ × 3H₂O (Sigma) as reported by Zanella et al. [19]. The Au loading was 2.8 wt% with a mean metal particle size determined by transition electron microscopy of 3.3 nm. Previous to use, the catalyst was in-situ activated under flow of O₂ (5%)/He (50 mL/min) at 250 °C for 60 min. The catalytic activity for methanol oxidation [CH₃OH (2700 ppm) + O₂ (20%)/He] was evaluated using a continuous plug-flow fixed bed microreactor at atmospheric pressure from room temperature (RT) to 250 °C. For each experiment, 50 mg of catalyst (40/60 mesh) diluted with 100 mg of quartz (100/120 mesh) was placed into the microreactor. The total flow was 100 mL/min. The outlet gas stream was analyzed continuously with a Prisma QMS 200 (Pfeiffer) mass spectrometer.

2.2 In situ and Modulation Excitation (ME) DRIFTS Experiments

Infrared spectroscopy in the diffuse reflectance (DRIFT) mode was used to investigate the adsorption and dynamic oxidation of methanol. A DRIFT cell (Harrick), with KBr windows, was mounted inside the sample compartment of the FTIR spectrometer (Thermo-Electron, Nicolet 8700 with a cryogenic MCT detector). The spectrometer bench was continuously purged with dried air (Parker Balston FTIR purge gas generator) to eliminate CO₂ and water vapor contributions to the spectra. Time-resolved IR spectra were recorded in kinetic mode at a resolution of 4 cm⁻¹. The background spectrum was collected without catalyst. The amount of catalyst used in the DRIFT cell was 50 mg, with a bed height of about 5–7 mm. The cell was connected to the feed gas cylinders through low-volume stainless-steel lines. Rapid exchange of the gas composition was performed by switching an electronically actuated flow-through valve (Vici-Valco Instruments), which prevents pressure drop during changes, synchronized with the FTIR spectrometer. The gas flows were set by mass flow controllers. The concentration of methanol in the gas feed was obtained by flowing He (3.5 mL/min) through a saturator containing liquid methanol at 5 °C. All the lines in contact with methanol were warmed to prevent condensation. Before methanol adsorption and

reaction, the catalyst was activated under flow of O₂ (5%)/He (50 mL/min) at 250 °C for 60 min, and then cooled down to 35 °C under He flow. The isothermal reaction of methanol oxidation [CH₃OH (2700 ppm) + O₂ (20%)/He, 100 mL/min] was studied between 35 to 200 °C at different temperatures on the preactivated catalysts. DRIFT spectra were collected at each temperature once a steady state of the infrared signal was reached (ca. 20 min). Next, isothermal concentration-modulation excitation spectroscopy (c-MES) experiments were performed [20]. After recording the background spectrum, a modulation experiment was started by varying the inlet gas composition from methanol (2700 ppm)/He to O₂ (20%)/He, while maintaining the same mass flow, using the desired modulation frequency. After allowing at least five modulation periods to adjust the system to the external perturbation the recording of the spectra was started. Spectra were acquired every 3 s, during each c-MES period, using reactants exchange frequency of 1.7 mHz. Phase sensitive detection (PSD) analysis of the spectra was performed according to the method developed by Baurecht and Fringeli [21]. More details on the technique can be found in reference [20] and in the Supplementary Information.

3 Theory

3.1 First Principles Calculations and Modeling

Density functional theory (DFT) calculations were performed with the real-space grid based GPAW code [22, 23] and the ASE simulation package [24]. The electron–electron exchange and correlation interactions were treated using the generalized gradient approximation (GGA) through the Perdew–Burke–Ernzerhof (PBE) functional. van der Waals interactions were also evaluated using the opt-PBE-vdW functional [25], the values for the adsorption of methanol and methoxy are reported in parentheses when corresponds. The core electrons are kept frozen and replaced by pseudopotentials generated by the plane augmented wave method (PAW). In all the calculations spin polarization was considered but no effect was found except for the system of O₂ in gas phase far from the stoichiometric TiO₂(110) surface. 3 × 3 × 1 k-points sampling and an uniform grid spacing of 0.2 Å were used. The Au/TiO₂ system was modeled by a (110) surface using a (2 × 3) supercell with four TiO₂ layers (Fig. 1). In all the calculations a vacuum corresponding to 25 Å was used to avoid image–image artificial interactions. For representation, the rutile structure has been selected due to its thermodynamic stability at ambient conditions. A gold particle deposited on a TiO₂ (110) surface was simulated by a cluster of four Au atoms, to maximized the metal-support interface for its analysis.

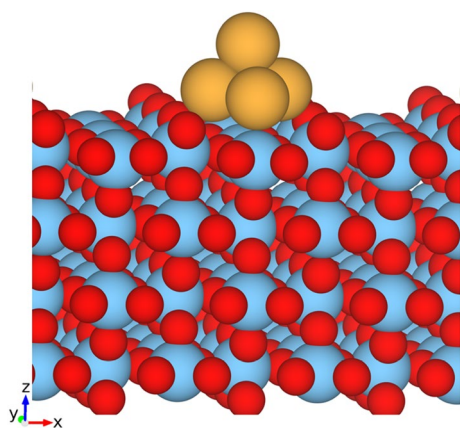


Fig. 1 Au cluster adsorbed on a TiO₂ rutile surface

Different adsorbates have been evaluated on several positions on the catalyst to analyze their behavior in the methanol oxidation mechanism. For all the systems, the two bottom layers were fixed at the next-neighbor distance corresponding to bulk and all the other layers and adsorbates were allowed to relax. For relaxations, the convergence criterion was achieved when the total forces were less than 0.05 eV/Å.

Two complementary sets of calculations were performed. First, we carried out a detailed vibrational analysis of the adsorbed species to provide valuable information about identification, the nature of the adsorption state and the dynamics of the surface process (see Tables S1 in the supporting information, SI). Vibrational frequency modes and energies for each species were calculated at the Γ -point within the harmonic approximations. Only the atoms of the adsorbates were allowed to vibrate. The force derivatives were calculated using the central difference approximation, with displacements of 0.03 Å. The method described in [26] has been followed to scale the computed frequencies. All the frequencies were scaled by a factor of 1.006, taking as a reference the calculated frequencies for the free methanol molecule with respect to the experimental values. Finally, the reaction mechanism for methanol oxidation were evaluated by the nudged elastic-band (NEB) method [27, 28] to find the minimum energy paths and the corresponding activation barriers using seven images of the system along the transition path. Within this method, the initial and final states are known and chain of beads is connected by harmonic springs ($k = 0.1$ eV/Å) between reactant and product states. Each transition state have been verified to have a single imaginary frequency. The general parameters used for the NEB calculations are the same as those for the previous DFT calculations described above.

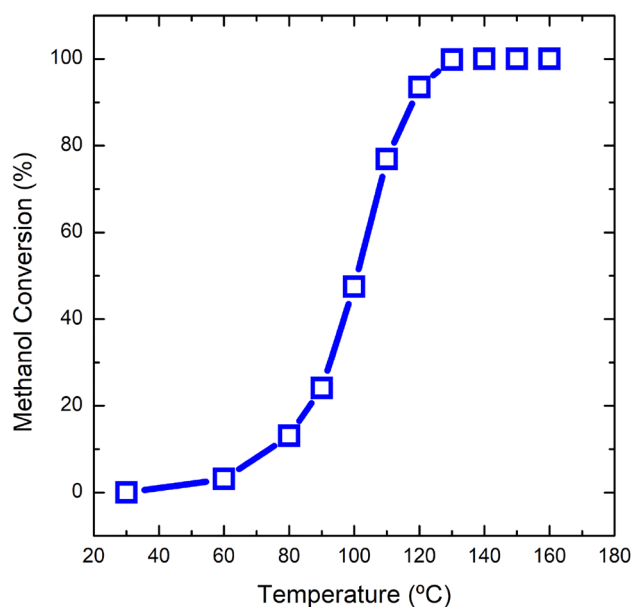


Fig. 2 Light off curve for the catalytic combustion of methanol on Au/TiO₂. Reaction conditions: CH₃OH (2700 ppm)/O₂ (20%)/He; total flow: 100 mL/min, catalyst weight: 50 mg

4 Results and Discussion

The oxidation of methanol on Au/TiO₂ has been investigated to evaluate the performance of the catalyst. Figure 2 depicts the light off curves for the combustion of methanol. It shows an onset of activity at ~ 50 °C, with 50% of conversion at 100 °C and a complete oxidation at 130 °C ($R_{\text{CH}_3\text{OH}} = 4.1 \mu \text{mol s}^{-1} \text{g}_{\text{cat}}^{-1}$). Similar performance under comparable reaction conditions was reported for Au/CeO₂ [29] and Au/TiO₂ [30].

To identify reaction intermediates, methanol adsorption on Au/TiO₂ has been dynamically investigated by DRIFT spectroscopy. After the activation treatment, the catalyst was cooled to the adsorption temperature and the gas flow was changed from pure He to CH₃OH (2700 ppm)/He. IR spectra were acquired every 1 s to monitor the dynamics of the adsorption process until the signals remained unchanged. Adsorption was carried out at 35 °C in order to avoid the decomposition of the adsorbed species. It should be noticed that there is no catalytic activity at this temperature.

Figure 3 presents the difference spectra during the exposure to methanol. During the adsorption, several bands increase in the 3000–2800 cm⁻¹ and 1600–1000 cm⁻¹ regions (Fig. 3(a)). It should be noted that some signals correspond to methanol in gas phase within the cell. For convenience, only those ones associated with adsorbed species will be referred. IR peaks corresponding to methanol (CH₃OH) and methoxy (CH₃O) adsorbed on TiO₂ have been assigned, and discussed below (Table 1). For verification,

Table 1 Experimental and theoretical vibrational frequencies for the adsorbed methanol and methoxy species

Vibrational mode	CH ₃ OH		CH ₃ O	
	Exp.	Theo.	Exp.	Theo.
$\nu(\text{OH})$	3500	3464	–	–
$\nu_{\text{as}}(\text{CH})$	2980	3058	2945	2952
$\nu_{\text{s}}(\text{CH})$	2837	2927	2820	2812
$\delta_{\text{as}}(\text{CH}_3)$	1430	1457	–	1436
$\delta_{\text{s}}(\text{CH}_3)$	1413	1434	–	1400
$\Gamma(\text{CH}_3)$	1163	1155	1140	1126
$\nu(\text{CO})$	1035	1036	1055	1142

Values are given cm^{-1}

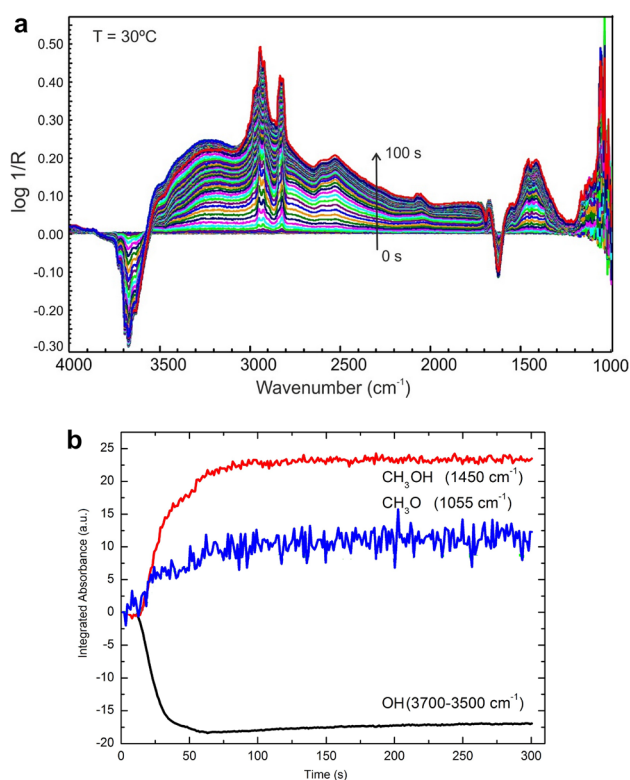


Fig. 3 **a** Infrared spectra collected during the adsorption of methanol (2700 ppm)/He on Au/TiO₂ at 30 °C, and **b** evolution of selected infrared signals during the methanol adsorption process

similar signals have been observed in an experiment employing a bare support, i.e. without gold (spectrum not shown). The assignment of IR signals corresponding to the surface species are displayed in Table 1. Our experimental and theoretical frequencies are in agreement with the ones reported in the literature [31–35]. Our results show:

i) For adsorbed methanol (CH₃OH) on Lewis acid sites, characteristic bands at 3500–3000 cm^{-1} [$\nu(\text{OH})$],

2980 cm^{-1} [$\nu_{\text{as}}(\text{CH})$], 2837 cm^{-1} [$\nu_{\text{s}}(\text{CH})$], 2920 cm^{-1} [$2 \times \delta_{\text{as}}(\text{CH}_3)$], 2897 cm^{-1} [$2 \times \delta_{\text{s}}(\text{CH}_3)$], 1430 cm^{-1} [$\delta_{\text{as}}(\text{CH}_3)$], 1413 cm^{-1} [$\delta_{\text{s}}(\text{CH}_3)$], 1163 cm^{-1} [$\Gamma(\text{CH}_3)$] and 1035 cm^{-1} [$\nu(\text{CO})$]; and

ii) For methoxy groups (CH₃O), on-top (linearly adsorbed) on a Ti site, characteristic bands at 2945 cm^{-1} [$\nu_{\text{as}}(\text{CH})$], 2820 cm^{-1} [$\nu_{\text{s}}(\text{CH})$], 2920 cm^{-1} [$2 \times \delta_{\text{as}}(\text{CH}_3)$], 2897 cm^{-1} [$2 \times \delta_{\text{s}}(\text{CH}_3)$], 1140 cm^{-1} [$\Gamma(\text{CH}_3)$] and 1055 cm^{-1} [$\nu(\text{CO})$].

Simultaneously with the growth of these signals, the decay of bands at 3700–3500 cm^{-1} and 1640 cm^{-1} was observed corresponding to surface OH species, which suggests that methanol adsorption occurs by reaction with surface hydroxyl groups [36]. Figure 3b shows the temporal evolution of selected signals corresponding to CH₃OH and CH₃O species. Similar results were reported by Nuhu et al. [16].

After completing the adsorption experiments, the gas flow was changed to the reaction mixture of CH₃OH (2700 ppm) + O₂ (20%)/He. Figures S1 and S2 (see Supporting Information) depict the steady state DRIFT spectra during the methanol oxidation between 50 and 250 °C for TiO₂ and Au/TiO₂, respectively. During the reaction, part of the bands due to methoxy species decrease as increasing the temperature. Simultaneously, sharp peaks at 2934 cm^{-1} , 2848 cm^{-1} , and 2721 cm^{-1} and in the low-frequency region, at 1665 cm^{-1} , 1595–1570 cm^{-1} and ca. 1378 cm^{-1} , 1358 cm^{-1} , typical of formate species (HCOO) accumulate in the surface of the Au/TiO₂ catalyst. In the bare support, similar bands are observed, but the oxidation of methoxy to formate is difficult in the absence of the metal particles.

Nevertheless, infrared signals during the steady state reaction at different temperatures exhibit a high level of spectral complexity, which makes almost impossible to differentiate between reaction intermediates and spectators. Thus, to identify and characterize the role of surface species during the reaction, c-MES experiments were performed at 100 °C on the Au/TiO₂ catalyst. This temperature was chosen because the catalyst exhibits a significant methanol conversion at that condition (see Fig. 1).

Figure 4a displays the time-resolved DRIFT spectra during a complete modulation cycle exchanging CH₃OH(2700 ppm)/He to O₂(5%)/He ($t = 120$ s). As expected, time-resolved DRIFT spectra showed modifications in the infrared bands, rather complex to analyze particularly in the fingerprint region between 1700 and 1000 cm^{-1} . Figure 4b presents the phase-domain spectra after applying the PSD algorithm, which allows a better observation of the spectral changes. The PSD method provides qualitative and quantitative information. The signals that are not affected by the applied stimulus are either very

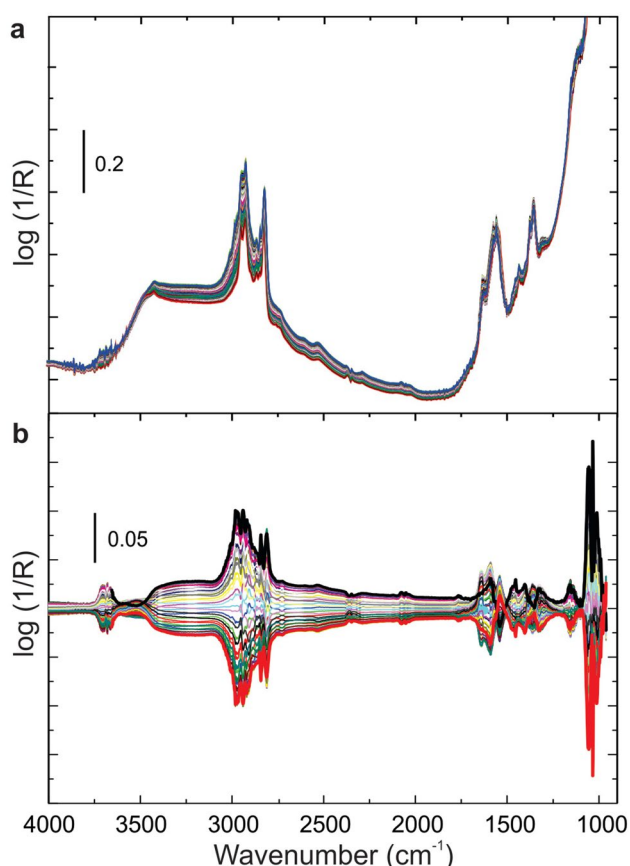


Fig. 4 **a** Time-domain DRIFT spectra during a c-MES cycle, $\text{CH}_3\text{OH}/\text{He}-\text{O}_2/\text{He}$ on the Au/TiO_2 catalyst. **b** Phase-domain spectra after PSD demodulation

slow (stable) intermediates or spectators. After applying the PSD algorithm, the signals corresponding to spectators are removed from the spectra along with the background, which greatly simplifies the analysis. Conversely, signals from species that are modified by the periodic perturbation, that is, reaction intermediates, are shown enhanced in the phase-resolved spectra. The phase delay (ϕ) with respect to the applied stimulus, that is, the phase angle at which the amplitude reaches a maximum, provides kinetic information about the role of the identified species. Therefore, the differentiation of species by means of phase delay of the surface species directly gives access to the reaction pathway of active species during a modulation period. Further details are provided in the supporting information and references therein. In the time-resolved spectra (Fig. 4a), most of the broad and intense peaks in the 1600–1200 cm^{-1} region remains almost constant during the modulated experiment. A similar observation can be made for the major part of the peaks at 2950–2800 cm^{-1} region, indicating that a fraction of methoxy and formate species (as will be discussed next) does not react and remains as spectator species. The phase delay (ϕ) with respect to the applied

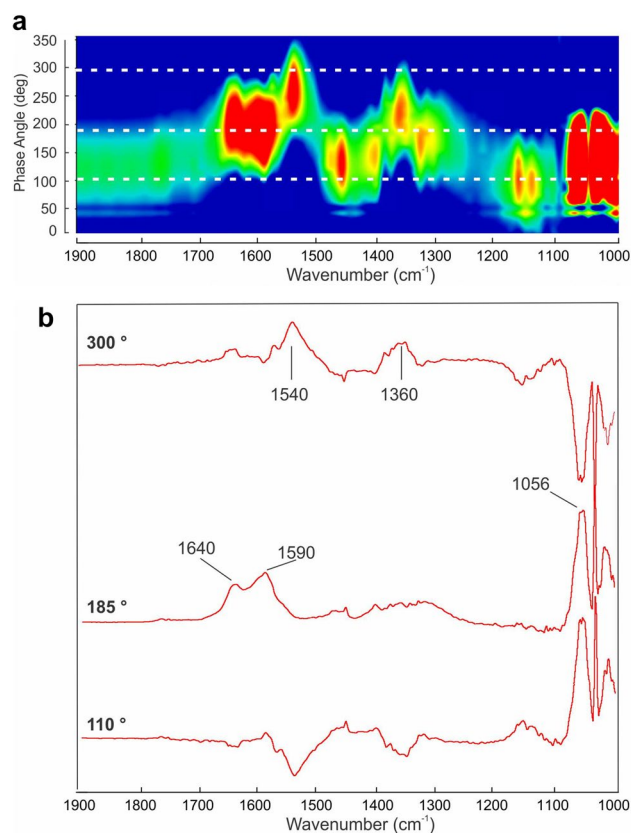


Fig. 5 **a** Two-dimensional iso-intensity map of the phase-resolved DRIFT spectra after PSD demodulation during a c-MES cycle, $\text{CH}_3\text{OH}/\text{He}-\text{O}_2/\text{He}$ on the Au/TiO_2 catalyst. **b** Phase-resolved spectra at selected phase lags

stimulus, that is, the phase angle at which the amplitude reaches a maximum, provides information about the role of the identified species.

For completeness, Fig. 5a shows the 2-D iso-intensity map spectra as a function of the phase lag (ϕ^{PSD}) and Fig. 5b displays some selected spectra. Synchronic signals can be easily observed by the emergence of red areas with the same phase lag. Surface species can be assigned to: methoxy (1056 cm^{-1} , $\phi = 110^\circ$), monodentate formate [m-HCOO] (1640 cm^{-1} , $\phi = 185^\circ$), bidentate formate [b-HCOO] (1590 cm^{-1} , $\phi = 185^\circ$) [37] and carbonate (1540 cm^{-1} , $\phi = 300^\circ$) adsorbed on titania [38]. Additionally, Fig. S3 (see Supporting Information) shows a signal assigned to CO adsorbed on gold sites, Au–CO (2115 cm^{-1} , $\phi = 275^\circ$), obtained at 100 $^\circ\text{C}$ [8].

It is important to note that the signals of surface species may be delayed with respect to oxygen (360°) or methanol (180°). Our results show that the methoxy species are in-phase with the entrance of methanol into the cell, whereas the formate groups, CO and carbonate are in-phase with the flow of oxygen. In other words, during the flow of

methanol, methoxy species are generated, and during the flow of oxygen, they are stepwise oxidized to CO₂.

With the aim to get a molecular understanding of the methanol oxidation reaction, modeling and optimization of feasible intermediate species adsorbed on a Au/TiO₂ surface during the methanol adsorption process have been performed by DFT. For all the species, the stability and vibrational modes have been evaluated, a detailed description can be found in the Supplementary Information (see Table S1). Particularly, for methanol and methoxy groups adsorbed on a TiO₂ surface, the calculated adsorption energies were -0.50 eV (-0.91 eV) and -2.57 eV (-2.67 eV), respectively. Results in agreement with reported data [39]. A comparison of these energy values confirm the weaker adsorption of methanol on the substrate, and the higher stability of the methoxy group on the surface. Thus, in most of the experimental and theoretical work, the O-H bond of methanol molecule is easily broken due to the lack of kinetic impediment, leading to a methoxy group and a H atom bonded to a neighboring O on the surface [39, 40]. Both species (CH₃OH and CH₃O) are found adsorbed by the oxygen atom to the Ti⁴⁺ (five-coordinate Ti atoms) of the TiO₂ surface according to [39, 40]. Additionally, theoretical vibrational frequencies have been calculated for adsorbed CH₃OH and CH₃O species, which are shown and compared with our experimental values in Table 1. It should be mentioned that except for the $\nu(\text{OH})$ mode that is absent in CH₃O, the other ones, which involve the methyl group such as $\nu(\text{CH})$, $\delta(\text{CH}_3)$ and $\Gamma(\text{CH}_3)$ remain almost unchanged when compared methyl groups and adsorbed methanol.

4.1 Methanol Reaction path to CO₂ on Au/TiO₂

To investigate the reaction path for methanol oxidation on Au/TiO₂ to produce CO₂ and H₂O, we combine the information obtained from our theoretical and experimental results. As a starting point and according to the evidence found in the literature [13, 14, 41–43], the presence of adsorbed OH and O species (labeled as OH_{ad} and O_{ad}) is detected on TiO₂ surfaces, scenario that has been taking into account for modeling (Fig. 6).

First, we have evaluated the molecular adsorption of methanol (1) and its consecutive reaction with a surface hydroxyl group (2), leading to the formation of methoxy and water in gas phase (3) in accord with our experimental findings (see the comparison in Table 1).

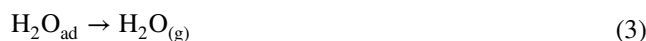
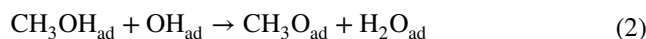
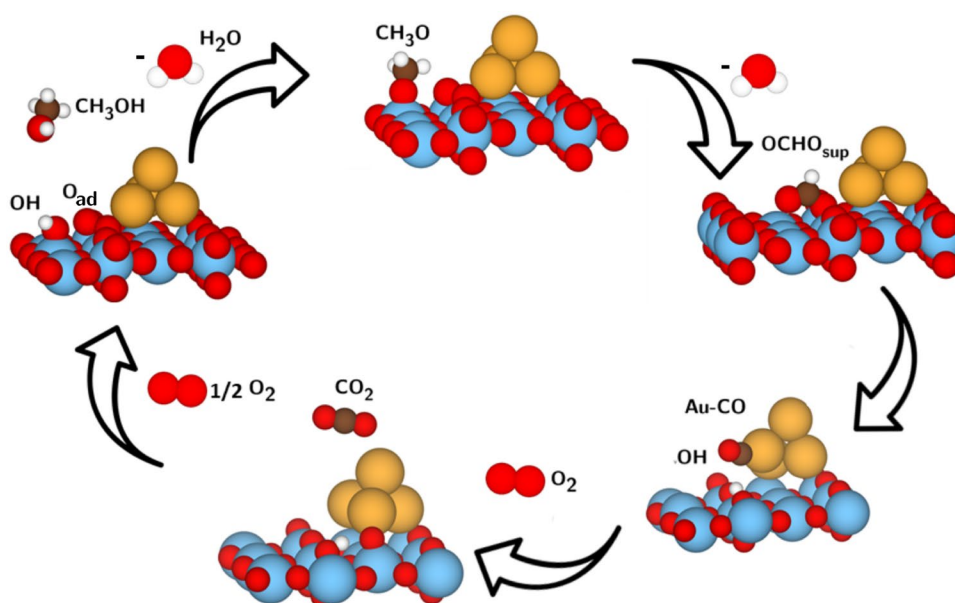


Figure 7 shows the path, which describes the first three steps. It can be observed that both, step 1 and step 2 are barrierless in agreement with [17], which involve the chemisorption of methanol on a Ti⁴⁺ top site next to an adsorbed OH group on the TiO₂ support, following by a hydrogen transfer from CH₃OH_{ad} to produce two adsorbed species, methoxy and water molecules. It was found that the desorption of water, step 3, exhibited an energy barrier of about 0.8 eV, in accordance with values reported in [17]. Steps 1, 2 and 3

Fig. 6 Proposed reaction mechanism for methanol oxidation on a Au/TiO₂ rutile surface. For simplicity, only the first surface layer of TiO₂ (110) is shown



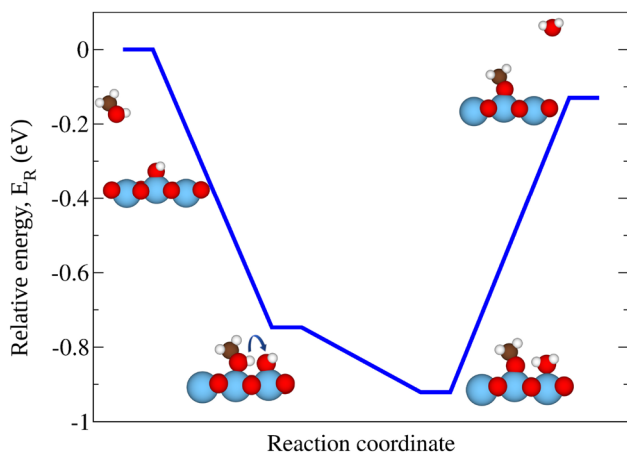
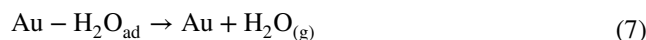
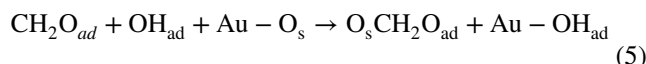
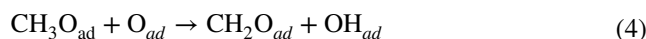


Fig. 7 Reaction path for steps 1, 2 and 3 involving CH₃OH adsorption on the Au/TiO₂ catalyst. The colored arrow is a help to the eye

are similar to experimental findings obtained by one of us in a previous work [30].

The reaction path continues with the oxidation of the methoxy intermediate, outlined by steps 4, 5, 6 and 7 (Fig. 8). First, the CH₃O_{ad} reacts with an O_{ad} leading to the formation of an adsorbed formaldehyde (CH₂O_{ad}) and a hydroxyl (OH_{ad}) species, both adsorbed on the titania support (4) with an activation energy of about 0.84 eV. Secondly, the reaction of the formaldehyde with a surface oxygen (i.e. a surface oxygen identified as O_s in the titania) to generate a dioxymethylene intermediate occurs with the concomitant migration of an OH_{ad} from the support to the gold cluster under barrierless conditions (5). Thirdly, the oxidation of O_sCH₂O_{ad} to a formate species via a hydrogen transfer produces an adsorbed water molecule on the Au cluster with an almost barrierless process (E_{act} of about 0.05 eV). Afterwards, water desorption takes place with an activation energy of ~ 0.38 eV (7). Formate species have been

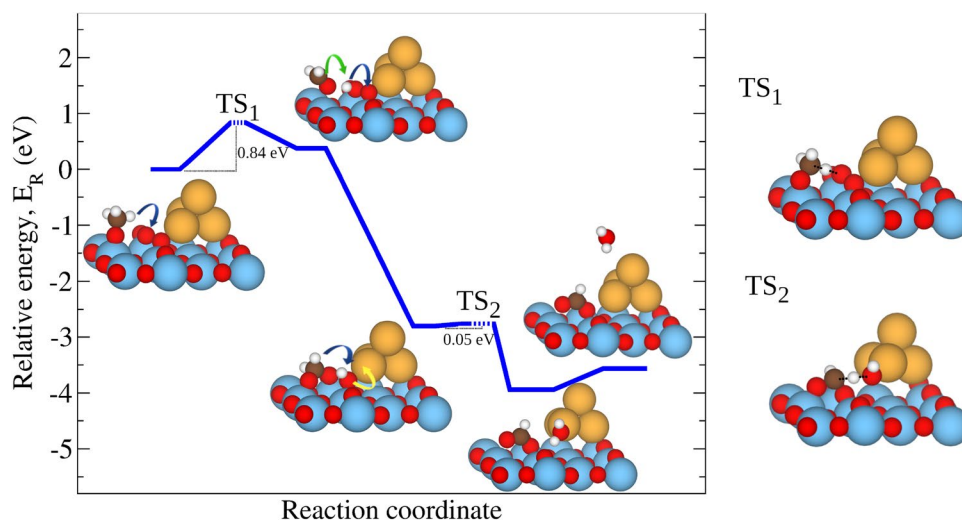
identified as reaction intermediates during the ME DRIFT experiments of methanol oxidation. Signals from adsorbed formaldehyde (or methylenebisoxo, O_sCH₂O_{ad}) were not registered during the infrared experiments due to the fast transformation to formate (barrierless process). In addition, it is worth to notice that the transformation of methoxy (CH₃O) to formate (HCOO) is a process mediated by the presence of gold nanoparticles on the titania surface, that is, almost no oxidation of methoxy are observed on the bare support (Figs. S1 and S2 in Supplementary Information).



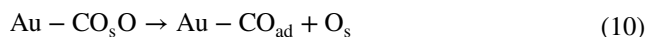
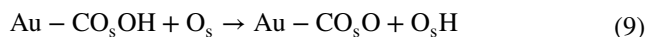
Experimental results show signals assigned to formate species at 2934 cm⁻¹ [$\nu(\text{CH})$], 2848 cm⁻¹ [$\nu_{as}(\text{OCO}) + \delta(\text{CH})$] and 2721 cm⁻¹ [$\nu_s(\text{OCO}) + \delta(\text{CH})$], 1640–1590 cm⁻¹ [$\nu_{as}(\text{OCO})$], and 1330 cm⁻¹ [$\nu_s(\text{OCO})$] [38, 44–46], which are in agreement with the theoretically modeled surface species (see Table S1). These infrared signals are generated after the change from methanol (methoxy) to oxygen (phase lag at 185°) in Fig. 5. It is important to notice that two synchronic bands are registered at 1640 cm⁻¹ and 1590 cm⁻¹. Both signals can arise from two different formate species, one of them can be compared with the vibrational modes of O_sCHO_{ad} ($\nu_{as}(\text{OCO}) = 1615 \text{ cm}^{-1}$) intermediate species at the interphase of gold–titania, although other species may be present as well.

The oxidation of O_sCHO_{ad}, detected as one of the products at step 6, leads to an adsorbed CO_{ad} on the Au

Fig. 8 Reaction path for steps 4, 5, 6 and 7 corresponding to the methoxy intermediate oxidation up to formation of formate species O_sCHO_{ad}. The colored arrows are a help to the eye. TS₁ and TS₂ identify transition state configurations, dotted lines represent the bond breaking and formation



cluster and a surface O_s in the titania. The reaction path is described by the following three steps (8, 9, 10):

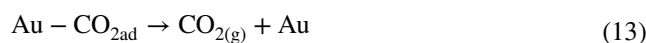


At this point, the effect of the Au-TiO₂ interface is clearly observed, where the oxidation of O_sCHO_{ad} occurs involving the Au cluster and the titania surface simultaneously. Specifically at step 8, the reaction of an adsorbed formate with gold is hindered by a barrier of about 0.26 eV. At the final state, a combined surface-cluster species ($Au - CO_sOH$) is observed with a carbon atom anchored to a gold atom and to a surface oxygen (Fig. 9). CO_sOH intermediate is similar to the carboxyl intermediate proposed as a key reaction intermediate during the water gas shift reaction [47–50]. Carboxyl species can be formed by the reaction of adsorbed CO with an OH group at the metal-support interface or by isomerization of a formate species [47, 50, 51]. Carboxyl species are regarded as very unstable intermediates, and therefore difficult to observe experimentally. Predicted frequencies are at 3385 cm⁻¹ [$\nu(OH)$], 1378 cm⁻¹ [$\nu_{as}(OCO)$], 1165 cm⁻¹ [$\nu_s(OCO)$] (Table S1, Supporting Information).

Subsequently, the $Au - CO_sOH$ oriented closer to a surface oxygen, starts a hydrogen transfer and the immediate bond formation of O_sH with the concomitant creation of $Au - CO_sO$. The process exhibits a low activation energy of 0.1 eV as displayed in Fig. 9. Finally, the C- O_s bond breaking in $Au - CO_sO$ produces $Au - CO_{ad}$ and recovers a O_s with a $E_{act} \approx 0.11$ eV (step 10, Fig. 9). This last process, in both directions (forward and backward), has been recently investigated in rather similar catalysts as part of the

low-temperature water gas shift mechanism [52], where barriers between (0.23–0.48) eV have been found. Experimentally, a weak signal due to Au-CO was registered during the ME DRIFT at 2115 cm⁻¹ (Fig. S3, Supporting Information), which is theoretically predicted as an intermediate of step 10 at $\nu(CO)$ at 2103 cm⁻¹ (Table S1, Supporting Information).

The last steps 11, 12 and 13 (Fig. 10), are well known and have been studied by other authors for years [53–56].



Experimentally, oxygen gas was incorporated into the chamber, therefore step 11 deals with the molecular adsorption of O₂ on the gold-support interface, with no barrier. Then, the adsorbed CO reacts with the neighboring molecular oxygen (O_{2ad}) ($E_{act} = 0.23$ eV) to produce CO_{2ad} on the gold cluster (step 12), which is released without an energy barrier in the next step (13). These results are in agreement with data reported in literature [55, 56], where O₂ adsorption and CO₂ desorption are barrierless processes, while CO oxidation near Au clusters shows barriers less than 0.3 eV. The CO oxidation reaction can proceed via two different reaction mechanisms: the Langmuir–Hinshelwood and the Au-assisted Mars van Krevelen mechanisms. In the first one, an adsorbed CO on a gold cluster reacts with adsorbed species (O₂ or O) localized at the interphase to produce CO₂ [7]. A detailed analysis can be found in [10]. In the second one, the CO on the Au cluster is oxidized by a lattice oxygen atom. This mechanism is observed only under oxidizing conditions, where additional O₂ molecules or O atoms are adsorbed at the interfacial region. A complete review about

Fig. 9 Reaction path for steps 8, 9 and 10 corresponding to the formate oxidation. The colored arrows are a help to the eye. TS₁, TS₂ and TS₃ identify transition state configurations

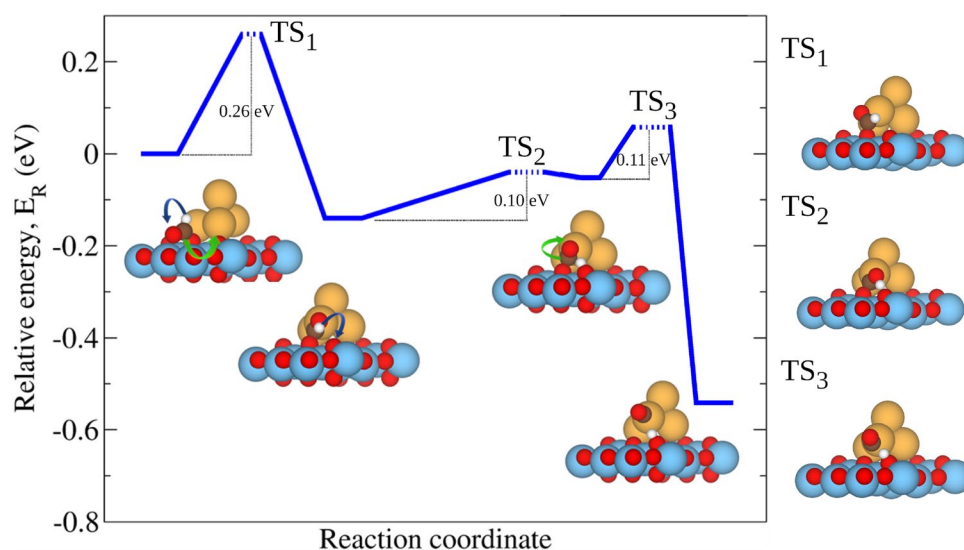
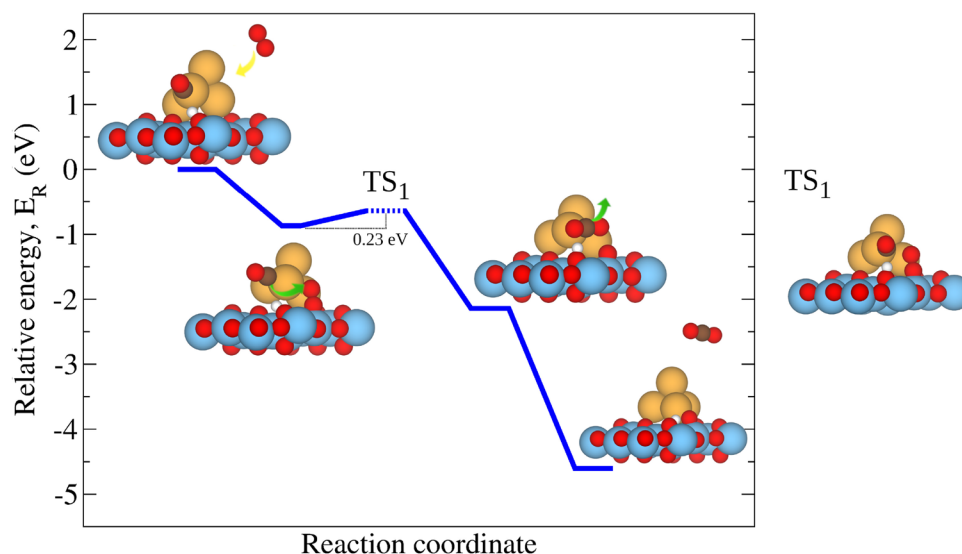


Fig. 10 Reaction path for steps 11 and 12 corresponding to the CO oxidation. The colored arrows are a help to the eye. TS₁ identifies a transition state configuration



the elemental steps of this mechanism is discussed by Pachioni and co-workers [11, 12].

Farnesi et al. [17, 18] performed a detailed DFT analysis of the partial oxidation of methanol on a Au₁₁/TiO₂(110) model system. They reported the adsorption of O₂ on the gold–titania interphase with an exothermic energy of -2.15 eV. Followed by the co-adsorption of a methanol molecule on the Au cluster (an Eley–Rideal type mechanism). The reaction produces a Au–CH₃O intermediate (an adsorbed methoxy on a gold site) involving the bond breaking of the O–O molecule with the formation of an OH on the titania surface, and an O_{ad} at the gold–titania interphase. Next, Au–CH₃O is oxidized, involving the donation of a H atom to the gold cluster ($E_a = 0.69$ eV), to CH₂O with a desorption energy of 0.29 eV. HREELS and temperature programmed experiments were performed in a ultrahigh vacuum (UHV) from -178 °C. They observed the evolution of formaldehyde with a peak at -21 °C. However, it is worth to notice that under methanol oxidation, formaldehyde is not observed and total selectivity to CO₂ is detected.

Beyond our proposal, it should be consider the possibility that CO_{2(g)} released in step 13 reacts with an O_{ad} or other surface species leading to the formation of adsorbed carbonate species, as reported in the literature [55]. Experimentally we observed a couple of bands at 1540 cm⁻¹ and 1360 cm⁻¹ (phase lag at 300°, Fig. 5). These signals are in accord with carbonate/carboxylate like species. Predicted bands of Au_{lat}-CO(O)O_s, at 1460 cm⁻¹ and 1285 cm⁻¹ (Table S1, Supporting Information) are close to the experimental observation. However, it is also possible that a carbonate/carboxylate species with a slightly different geometry appears, which could generate an important shift in the vibrational frequencies as reported in Table S1.

Finally, for completeness, the catalytic cycle is closed following steps 14 and 15.



5 Conclusions

In this study, we have examined the total CH₃OH oxidation on Au/TiO₂ catalyst. Combining in situ MES-DRIFT experiments and periodic DFT calculations a detailed picture of the reaction mechanism is presented. Methanol is adsorbed on the titania surface as methoxy species. Only a minor part of the adsorbed species is oxidized on gold-support sites at the interface, that is, adsorbed species on TiO₂ far from the metal particles remain as spectators. A stepwise oxidation of methoxy proceeds through methylentebisoxo (adsorbed formaldehyde), formate, carboxyl and CO. Methoxy oxidation is regarded as the rate-limiting step. The role of the metal-support interface is highlighted for the oxidation of the carbonaceous intermediates as well for the activation of molecular oxygen.

Supplementary Information The online version contains supplementary material available at <https://doi.org/10.1007/s11244-022-01620-7>.

Acknowledgements Financial support by CONICET and Universidad Nacional del Litoral is gratefully acknowledged. G.D.B, N.C., E.C. and P.Q. thanks PICT-2017-1342 and PICT-2019-03392 for support. S.C. acknowledges PICT-2018-01332. The authors also thank the support given by Santa Fe Science Technology and Innovation Agency (ASACTEI, Grant No. 00010-18-2014).

References

- Kamal MS, Razzak SA, Hossain MM (2016) Catalytic oxidation of volatile organic compounds (VOCs). A review. *Atmos Environ* 140:117–134
- Pilasombat R, Daly H, Goguet A, Breen J, Burch R, Hardacre C, Thompsett D (2012) Investigation of the effect of the preparation method on the activity and stability of Au/CeZrO₄ catalysts for the low temperature water gas shift reaction. *Catal Today* 180(1):131–138
- Scirè S, Liotta LF (2012) Supported gold catalysts for the total oxidation of volatile organic compounds. *Appl Catal B Environ* 125:222–246
- Scirè S, Riccobene PM, Crisafulli C (2010) Ceria supported group IB metal catalysts for the combustion of volatile organic compounds and the preferential oxidation of CO. *Appl Catal B Environ* 101(1–2):109–117
- Delannoy L, Fajerweg K, Lakshmanan P, Potvin C, Methivier C, Louis C (2010) Supported gold catalysts for the decomposition of VOC: total oxidation of propene in low concentration as model reaction. *Appl Catal B Environ* 94(1–2):117–124
- Petrova P, Tabakova T, Munteanu G, Zanella R, Tsvetkov M, Ilieva L (2013) Gold catalysts on Co-doped ceria for complete benzene oxidation: relationship between reducibility and catalytic activity. *Catal Commun* 36:84–88
- Green IX, Tang W, McEntee M, Neurock M, Yates Jr JT (2012) Inhibition at perimeter sites of Au/TiO₂ oxidation catalyst by reactant oxygen. *J Am Chem Soc* 134(30):12717–12723
- Green IX, Tang W, Neurock M, Yates JT (2011) Spectroscopic observation of dual catalytic sites during oxidation of CO on a Au/TiO₂ catalyst. *Science* 333(6043):736–739
- Sun K, Kohyama M, Tanaka S, Takeda S (2017) Reaction mechanism of the low-temperature water–gas shift reaction on Au/TiO₂ catalysts. *J Phys Chem C* 121(22):12178–12187
- Wang YG, Yoon Y, Glezakou VA, Li J, Rousseau R (2013) The role of reducible oxide–metal cluster charge transfer in catalytic processes: new insights on the catalytic mechanism of CO oxidation on Au/TiO₂ from ab initio molecular dynamics. *J Am Chem Soc* 135(29):10673–10683
- Schlexer P, Widmann D, Behm RJ, Pacchioni G (2018) Co oxidation on a Au/TiO₂ nanoparticle catalyst via the Au-assisted Mars-van Krevelen mechanism. *ACS Catal* 8(7):6513–6525
- Tosoni S, Pacchioni G (2019) Oxide-supported gold clusters and nanoparticles in catalysis: a computational chemistry perspective. *ChemCatChem* 11(1):73–89
- Bazin P, Thomas S, Marie O, Daturi M (2012) New insights into the methanol oxidation mechanism over Au/CeO₂ catalyst through complementary kinetic and FTIR operando SSITKA approaches. *Catal Today* 182(1):3–11
- Rousseau S, Marie O, Bazin P, Daturi M, Verdier S, Harlé V (2010) Investigation of methanol oxidation over Au/catalysts using operando IR spectroscopy: determination of the active sites, intermediate/spectator species, and reaction mechanism. *J Am Chem Soc* 132(31):10832–10841
- Kähler K, Holz MC, Rohe M, van Veen AC, Muhler M (2013) Methanol oxidation as probe reaction for active sites in Au/ZnO and Au/TiO₂ catalysts. *J Catal* 299:162–170
- Nuhu A, Soares J, Gonzalez-Herrera M, Watts A, Hussein G, Bowker M (2007) Methanol oxidation on Au/TiO₂ catalysts. *Top Catal* 44:293–297
- Farnesi Camellone M, Marx D (2014) Nature and role of activated molecular oxygen species at the gold/titania interface in the selective oxidation of alcohols. *J Phys Chem C* 118(36):20989–21000
- Farnesi Camellone M, Zhao J, Jin L, Wang Y, Muhler M, Marx D (2013) Molecular understanding of reactivity and selectivity for methanol oxidation at the Au/TiO₂ interface. *Angew Chem Int Ed* 52(22):5780–5784
- Zanella R, Louis C (2005) Influence of the conditions of thermal treatments and of storage on the size of the gold particles in Au/TiO₂ samples. *Catal Today* 107:768–777
- Aguirre A, Collins S (2013) Selective detection of reaction intermediates using concentration-modulation excitation DRIFT spectroscopy. *Catal Today* 205:34–40
- Baurecht D, Fringeli U (2001) Quantitative modulated excitation fourier transform infrared spectroscopy. *Rev Sci Instrum* 72(10):3782–3792
- Enkovaara JE, Rostgaard C, Mortensen J et al (2010) Electronic structure calculations with GPAW: a real-space implementation of the projector augmented-wave method. *J Phys Condens Matter* 22(25):253202
- Mortensen JJ, Hansen LB, Jacobsen KW (2005) Real-space grid implementation of the projector augmented wave method. *Phys Rev B* 71(3):035109
- Larsen A, Mortensen J, Blomqvist J, Castelli I, Christensen R, Dułak M, Friis J, Groves M, Hammer B, Hargus C, Hermes E, Jennings P, Jensen P, Kermode J, Kitchin J, Kolsbjerg EL, Kubal J, Kaasbjerg K, Lysgaard S, Maronsson J, Maxson T, Olsen T, Pastewka L, Peterson A, Rostgaard C, Schiøtz J, Schütt O, Strange M, Thygesen K, Vegge T, Vilhelmsen L, Walter M, Zeng Z, Jacobsen K (2017) The atomic simulation environment—a Python library for working with atoms. *J Phys Condens Matter* 29(27):273002
- Klimeš J, Bowler D, Michaelides A (2010) Chemical accuracy for the van der waals density functional. *J Phys Condens Matter* 22(022):201
- Ma X, Genest A, Spanu L, Rösch N (2015) Structures and vibrational frequencies of CO adsorbed on transition metals from calculations using the vdW-DF2 functional. *Comput Theoret Chem* 1069:147
- Henkelman G, Uberuaga BP, Jónsson H (2000) A climbing image nudged elastic band method for finding saddle points and minimum energy paths. *J Chem Phys* 113(22):9901–9904
- Henkelman G, Jónsson H (2000) Improved tangent estimate in the nudged elastic band method for finding minimum energy paths and saddle points. *J Chem Phys* 113(22):9978–9985
- Scirè S, Minico S, Crisafulli C, Satriano C, Pistone A (2003) Catalytic combustion of volatile organic compounds on gold/cerium oxide catalysts. *Appl Catal B Environ* 40(1):43–49
- Calzada LA, Collins SE, Han CW, Ortalan V, Zanella R (2017) Synergetic effect of bimetallic Au–Ru/TiO₂ catalysts for complete oxidation of methanol. *Appl Catal B Environ* 207:79–92
- Derouault J, Le Calve J, Forel M (1972) Discussion des vibrations de valence $\nu(\text{CH}_3)$ and $\nu(\text{CD}_3)$ des groupes OCH₃ and OCD₃: influence de la formation d'une liaison de coordination entre l'oxygène et les halogénures d'aluminium ou le trifluorure de bore. *Spectrochim Acta Part A Mol Spectrosc* 28(2):359–371
- Lavalley J, Sheppard N (1972) Anharmonicity of CH₃ deformation vibrations and fermi resonance between the symmetrical CH₃ stretching mode and overtones of CH₃ deformation vibrations. *Spectrochim Acta Part A Mol Spectrosc* 28(11):2091–2101
- Bellamy LJ (1968) *Advances in infrared group frequencies*. Methuen & Co, London
- Collins S, Briand L, Gambaro L, Baltanas M, Bonivardi A (2008) Adsorption and decomposition of methanol on gallium oxide polymorphs. *J Phys Chem C* 112(38):14988–15000
- Lavalley J (1996) Infrared spectrometric studies of the surface basicity of metal oxides and zeolites using adsorbed probe molecules. *Catal Today* 27(3):377–401
- Burcham LJ, Badlani M, Wachs IE (2001) The origin of the ligand effect in metal oxide catalysts: novel fixed-bed in situ infrared and kinetic studies during methanol oxidation. *J Catal* 203(1):104–121

37. Mattsson A, Österlund L (2017) Co-adsorption of oxygen and formic acid on rutile TiO_2 (110) studied by infrared reflection-absorption spectroscopy. *Surf Sci* 663:47–55
38. Busca G, Lorenzelli V (1982) Infrared spectroscopic identification of species arising from reactive adsorption of carbon oxides on metal oxide surfaces. *Mater Chem* 7(1):89–126
39. Zhao J, Yang J, Petek H (2009) Theoretical study of the molecular and electronic structure of methanol on a TiO_2 (110) surface. *Phys Rev B* 80(23):235,416
40. Sanchez De Armas R, Oviedo J, San Miguel M, Sanz J (2007) Methanol adsorption and dissociation on TiO_2 (110) from first principles calculations. *J Phys Chem C* 111(27):10023–10028
41. Du Y, Deskins NA, Zhang Z, Dohnálek Z, Dupuis M, Lyubinskiy I (2009) Imaging consecutive steps of O_2 reaction with hydroxylated TiO_2 (110): identification of HO_2 and terminal OH intermediates. *J Phys Chem C* 113(2):666–671
42. Henderson MA, Epling WS, Peden C, Perkins CL (2003) Insights into photoexcited electron scavenging processes on TiO_2 obtained from studies of the reaction of O_2 with OH groups adsorbed at electronic defects on TiO_2 (110). *J Phys Chem B* 107(2):534–545
43. Tilocca A, Di Valentin C, Selloni A (2005) O_2 interaction and reactivity on a model hydroxylated rutile (110) surface. *J Phys Chem B* 109(44):20963–20967
44. Li C, Domen K, Maruya KI, Onishi T (1990) Oxygen exchange reactions over cerium oxide: an FT-IR study. *J Catal* 123(2):436–442
45. Binet C, Daturi M, Lavalley JC (1999) IR study of polycrystalline ceria properties in oxidised and reduced states. *Catal Today* 50(2):207–225
46. Collins SE, Baltanas MA, Bonivardi AL (2004) An infrared study of the intermediates of methanol synthesis from carbon dioxide over $\text{Pd}/\beta\text{-Ga}_2\text{O}_3$. *J Catal* 226(2):410–421
47. Chen Y, Wang H, Burch R, Hardacre C, Hu P (2011) New insight into mechanisms in water-gas-shift reaction on Au/CeO_2 (111): a density functional theory and kinetic study. *Faraday Discuss* 152:121–133
48. Gong XQ, Hu P, Raval R (2003) The catalytic role of water in CO oxidation. *J Chem Phys* 119(12):6324–6334
49. Liu ZP, Jenkins SJ, King DA (2005) Origin and activity of oxidized gold in water-gas-shift catalysis. *Phys Rev Lett* 94(19):196102
50. Mudiyansele K, Senanayake SD, Feria L, Kundu S, Baber AE, Graciani J, Vidal AB, Agnoli S, Evans J, Chang R et al (2013) Importance of the metal-oxide interface in catalysis: In situ studies of the water-gas shift reaction by ambient-pressure X-ray photoelectron spectroscopy. *Angew Chem Int Ed* 52(19):5101–5105
51. Vecchiotti J, Bonivardi A, Xu W, Stacchiola D, Delgado JJ, Calatayud M, Collins SE (2014) Understanding the role of oxygen vacancies in the water gas shift reaction on ceria-supported platinum catalysts. *ACS Catal* 4(6):2088–2096
52. Yin P, Yu J, Wang L, Zhang J, Jie Y, Chen LF, Zhao XJ, Feng HS, Yang YS, Xu M et al (2021) Water-gas-shift reaction on $\text{Au}/\text{TiO}_{2-x}$ catalysts with various TiO_2 crystalline phases: a theoretical and experimental study. *J Phys Chem C* 125(37):20360–20372
53. Wang YG, Cantu DC, Lee MS, Li J, Glezakou VA, Rousseau R (2016) CO oxidation on Au/TiO_2 : condition-dependent active sites and mechanistic pathways. *J Am Chem Soc* 138(33):10467–10476
54. Chrétien S, Metiu H (2008) Enhanced adsorption energy of Au_1 and O_2 on the stoichiometric TiO_2 (110) surface by coadsorption with other molecules. *J Chem Phys* 128(4):044714
55. Koga H, Tada K, Okumura M (2015a) DFT study of CO oxidation catalyzed by Au/TiO_2 : Activity of small clusters. *e-Journal of Surface Science and Nanotechnology* 13:129–134
56. Koga H, Tada K, Okumura M (2015b) Density functional theory study of active oxygen at the perimeter of Au/TiO_2 catalysts. *J Phys Chem C* 119(46):25907–25916

Publisher's Note Springer Nature remains neutral with regard to jurisdictional claims in published maps and institutional affiliations.